IOP Conf. Series: Materials Science and Engineering **297** (2018) 012012 doi:10.1088/1757-899X/297/1/012012

Viscous investigation of a flapping foil propulsor

Attapol Posri, Surasak Phoemsapthawee* and Nonthipat Thaweewat

Department of Maritime Engineering, Faculty of International Maritime Studies, Kasetsart University, Thailand

* Corresponding Author: surasak.pho@ku.th

Abstract. Inspired by how fishes propel themselves, a flapping-foil device is invented as an alternative propulsion system for ships and boats. The performance of such propulsor has been formerly investigated using a potential flow code. The simulation results have shown that the device has high propulsive efficiency over a wide range of operation. However, the potential flow gives good results only when flow separation is not present. In case of high flapping frequency, the flow separation can occur over a short instant due to fluid viscosity and high angle of attack. This may cause a reduction of propulsive efficiency. A commercial CFD code based on Lattice Boltzmann Method, XFlow, is then employed in order to investigate the viscous effect over the propulsive performance of the flapping foil. The viscous results agree well with the potential flow results, confirming the high efficiency of the propulsor. As expected, viscous results show lower efficiency in high flapping frequency zone.

1. Introduction

Flying and swimming creatures have transformed their organs into flapping foils, for example, wings, fins or tails [1], to propel themselves. After million years of evolution, the hydrodynamic optimization of such flapping foil propulsor is obtained through natural selection [2]. Undoubtedly, this biomimetic propulsor interests inventors to use it as a propulsion system. Several numerical and experimental studies have been performed to clarify the flapping foil mechanism [3, 4,5]. This illuminates the way to use a flapping foil as a ship propulsion system. A study based on Boundary Element Method [6] has concluded that a flapping foil can be used as a marine propulsive device since its performance is comparable to a conventional marine propeller. However, the efficiency of the flapping foil used as an energy harvesting device has been reported to be lower than that of a rotary turbine [7].

In order to explore the parametric space of flapping foil mechanism, especially the kinematics giving optimal propulsive efficiency, researches using two-dimensional or three-dimensional Boundary Element Method have been performed to study effects of foil motions, for example angle of attack profile [8], or geometry [9]. Moreover, by attaching a flapping foil beneath ship hull either vertically or horizontally, the ship response in waves can be improved [10, 11]. Significant trust as well as anti-rolling improvement has been reported. It can simply be said that the overall ship performance is enhanced.

In an effort to use a flapping foil as a ship propulsive device, the efficiency of flapping foil has been calculated using potential flow theory and presented similarly to that of screw propeller series [6]. The transition between the two regimes, e.g., flapping foil and marine propeller, has been done by introducing an equivalent advance ratio. Another pattern in matching the propulsive foil and prime mover power has been presented [12]. A numerical study based on potential flow method [13] has

presented a complete openwater characteristics of flapping foil. Such information is necessary for matching and optimizing the ship propulsion system.

The linear theory and inviscid numerical method, i.e., Boundary Element Method (BEM) is mentioned as a useful tool for hydrodynamic force prediction at high Reynolds numbers [9]. However, these inviscid methods can sometimes lead to disagreement of results in comparison with those of experiments or viscous solver at a certain range of dimensionless number describing flapping frequency such as reduced frequency, Strouhal number or advance number.

Due to a lack of boundary layer model in potential method, the results of inviscid simulation may slightly deviate from reality of physical flow. In the present study, the hydrodynamic force coefficients and propulsive efficiency obtained from inviscid model [13] will be compared to that of viscous solver. The results are presented as functions of equivalent advance number in order to be comparable to marine propeller.

2. Flapping Foil Propulsor

In this section the mechanism of flapping foil propulsor as well as the openwater characteristics is defined. In order to investigate the viscous effect over the openwater characteristics reported in [13], a flapping foil with NACA0012 section and an aspect ratio of 5 is simulated. The nomenclature in this paper is defined following the work in [13].

2.1. *Flapping Motion*

The flapping mechanism can be described by two sinusoidal motions: the heave and the pitch motions as presented in equation (1) and (2) respectively.

$$h = h_0 \sin(2\pi f t + \frac{\pi}{2}) \tag{1}$$

$$\theta = \theta_0 \sin(2\pi f t + \pi) \tag{2}$$

where h is the heave position, h_0 is the heave amplitude, θ is the pitch angle, θ_0 is the pitch amplitude or in the other hand the maximum pitch angle, f is the motion frequency. The heave and the pitch motions are defined at the middle of the chord as illustrated in figure 1.

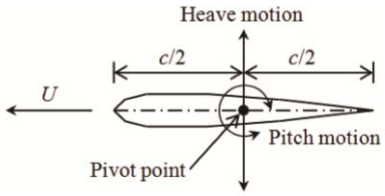

Figure 1. Definition of the flapping motion (reproduced from [13]).

2.2. *Openwater Characteristics*

Openwater characteristics are the performance of a propulsor in a uniform flow. Following the work [13], the openwater characteristics of a flapping foil propulsor consist of four non-dimensional parameters: the thrust coefficient K_T, the heave-force coefficient K_H, the pitch-moment coefficient K_P and the propulsive efficiency η. The definitions of all force coefficients are described as follow:

$$K_T = \frac{\overline{T}}{\rho f^2 D_{eq}{}^4} \tag{3}$$

$$K_H = \frac{H_{\max}}{\rho f^2 D_{eq}{}^4} \tag{4}$$

$$K_P = \frac{P_{\max}}{\rho f^2 D_{eq}^5} \tag{5}$$

where $\overline{T}$ is the average thrust, $H_{\max}$ is the maximum heave force, $P_{\max}$ is the maximum pitch moment, ρ is the fluid density. Since the flapping foil propulsor has been represented as a screw propeller, the reference length is defined as an equivalent diameter $D_{eq} = \sqrt{8h_0 b/\pi}$ where b is the foil span.

The propulsive efficiency η of a flapping foil propulsor is the ratio between the propulsive power and the input power used to drive the flapping motion over a flapping period:

$$\eta = \frac{U\overline{T}}{f\int_0^{1/f}\left(H\dot{h} + P\dot{\theta}\right)dt} \tag{6}$$

where U is the advance velocity, H is the heave force, $\dot{h}$ is the heave velocity, P is the pitch moment, $\dot{\theta}$ is the pitch angular velocity.

All of these openwater parameters are presented as functions of a dimensionless number describing the flapping frequency which is represented in this paper as an equivalent advance number J_{eq}.

$$J_{eq} = \frac{U}{f D_{eq}} \tag{7}$$

3. Simulation Tool Investigation

A commercial CFD code based on Lattice Boltzmann Method, XFlow 2016, is used to simulate the flow around flapping foil since the solver is effectively capable to work with moving object and reduce time in meshing process due to its automatic mesh generation (AMG) [14]. The solver has characteristics of Wall-Modeled Large Eddy Simulation which is applied for turbulence modeling and near-wall treatment [15, 16].

A small number of works has been done to clarify the influence of boundary domain. In order to optimize the computational expense while still possessing acceptable accuracy of the numerical results, the domain size, as well as resolutions of near wall and wake, is examined, in the same way as meshing sensitivity of conventional CFD is performed. Simulations of a simple lifting problem, a foil with an incident angle, are then performed. The simulation tool investigation is broken into two scenarios: the resolution convergence problem and the domain size problem.

The initial domain is imposed in term of chord length. The boundary condition is setup as depicted in figure 2. The size of initial domain is defined similarly to the work in [17]. The simulations employ a mirror technique since the flow is symmetric at the mid span plane. A NACA 0012 foil is then placed at the free-slip wall. The angle of attack of the foil is set to be 5 degrees. The simulations are performed with a Reynold number of 1 million.

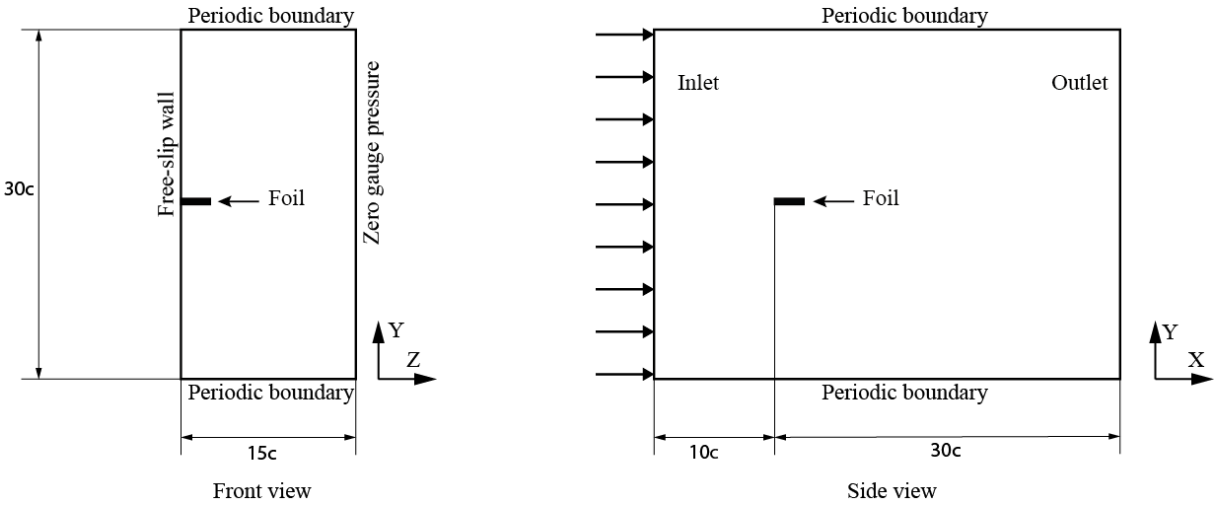

Figure 2. Initial computational domain**.**

3.1. *Resolution Convergence*

The resolution convergence is investigated as a function of the lattice size over the chord length. The resolutions of wall and wake region are set to be equal. The far-field resolution is always set to equal to the chord length. The adaptive resolution scheme is employed to vary the lattice size from the wall and wake regions to the far-field conditions. The investigation results are shown in figure 3 and as the computation times are shown in table 1.

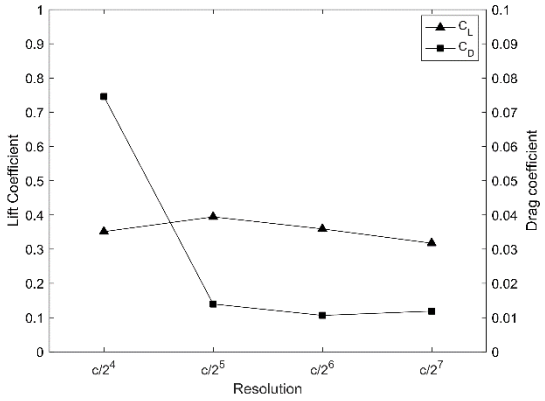

Figure 3. Lift and drag coefficients against simulation resolution.

Table 1. Simulation time in function of resolution.

Resolution	Time
$c/2^4$	8 mins.
$c/2^5$	38 mins.
$c/2^6$	3 hrs. 31 mins.
$c/2^7$	>25hrs.

According to figure 3, the resolution of $c/2^5$ is chosen to be the optimized resolution since both lift and drag coefficients do not change significantly with higher resolutions. Table 1 also indicates that the computation time increases exponentially as a function of resolution.

3.2. *Simulation Domain*

Although, XFlow has been used to simulate a flapping foil [18], the domain size investigation has not been presented. A proper domain size used to simulate the NASA trapezoidal wing [17] has been suggested in which the wall effect is negligible on the basis of a small blockage ratio. However, the domain size for foil is examined in this section.

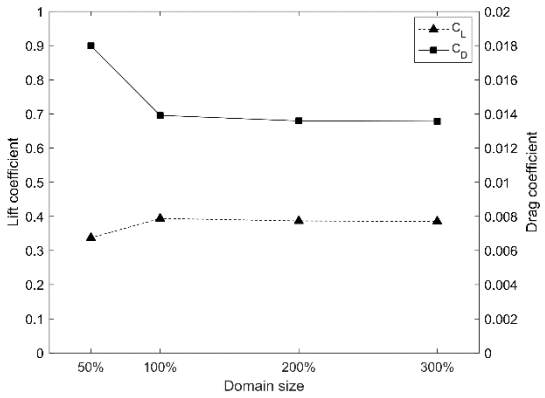

Figure 4. Lift and drag coefficient against domain size with respect to the initial domain size.

Table 2. Simulation time in function of domain size with respect to the initial domain size.

Domain size	Time
50%	47 mins.
100%	42 mins.
200%	44 mins.
300%	45 mins.

Figure 4 show the influence of the domain size in percentage of the initial domain. Although, the domain size of 100% of the initial one seems to be sufficient to accurately simulate the foil, the domain size of 200% is selected to simulate the flapping foil since the time-consuming unnoticeably changes as the domain is varied. Also, the flow physics of flapping foil is considerably different from that of a stationary wing due to its kinematics that creates an obstruction area.

4. Results and Discussion

Whilst the presence of a von Karman street coincides with drag generation, the presence of a reverse von Karman street coincides with thrust generation as illustrated in [6]. These phenomena agree very well with the change of fluid momentum. An example of vorticity distribution in the wake zone of the XFlow simulations illustrating a reverse von Karman street is present in figure 5. However, the reverse Von Karman cannot be directly implied from figure 5 since unfortunately XFlow presents vorticity in absolute value.

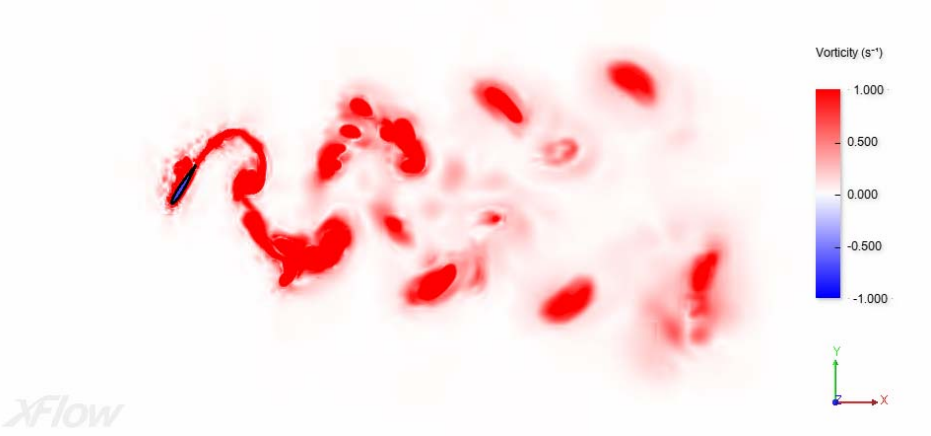

Figure 5. Example of vorticiy distribution in wake zone illustrating a reverse von Karman street.

The simulation results with the viscous effect are compared to those of potential flow theory. It can be seen from figure 6 to 9 that the results of the two methods give a good agreement for both propulsive efficiency and thrust coefficient in spite of noticeable deviations especially for kinematics with pitch amplitude of 15 degrees. At this small pitch, the viscous solver tends to give lower thrust as well as propulsive efficiency for all heave-to-chord ratio in comparison with those of BEM. For moderate pitch, e.g. θ_0 = 30° and 45°, the LBM seemingly gives a slightly higher propulsive efficiency, except for the very high heave-to-chord ratio (h_0/c = 4).

In addition, for each pitch amplitude, the difference of simulation results from both method is higher with a lower advance number. This is expectable since a lower advance number, or in other word a higher flapping frequency, corresponds to a higher angle of attack. The viscous effect undoubtedly has more influence in this zone.

Figure 10 to 13 present the comparison of heave-force and pitch-moment coefficients between the two methods. The numerical results agree very well especially for high heave-to-chord ratio. Although the deviation for the case of 15° pitch amplitude is visually noticeable, the ratio between the two results is not much different compared to the other cases of pitch amplitude. The deviation are more clearly seen on the pitch-moment coefficient with low heave-to-chord ratio and high pitch amplitude.

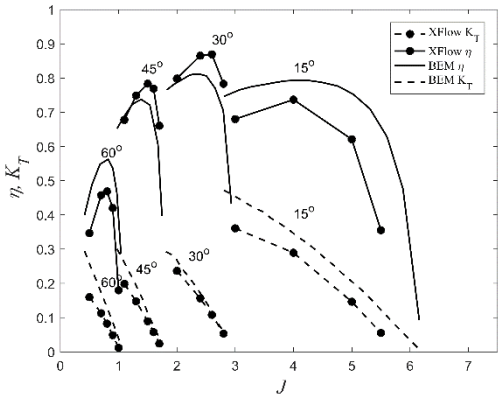

Figure 6. K_T and η in function of J_{eq}; h_0/c = 1; θ_0 = 15°, 30°, 45° and 60°.

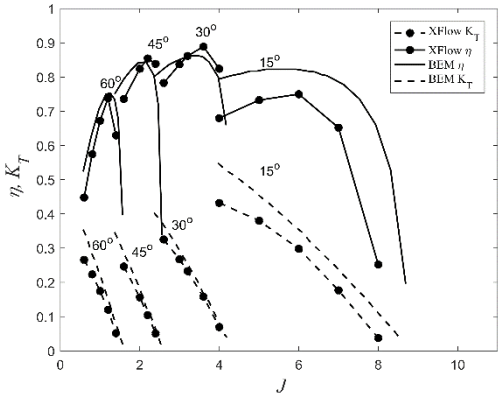

Figure 7. K_T and η in function of J_{eq}; h_0/c = 2; θ_0 = 15°, 30°, 45° and 60°.

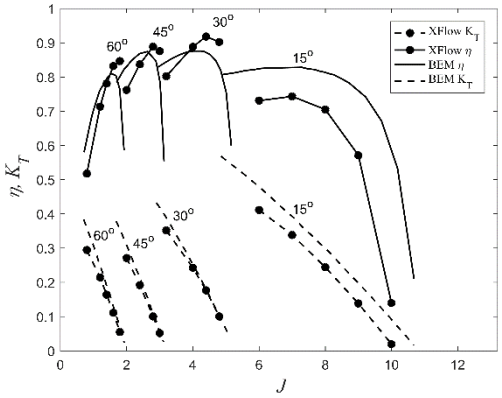

Figure 8. K_T and η in function of J_{eq}; h_0/c = 3; θ_0 = 15°, 30°, 45° and 60°.

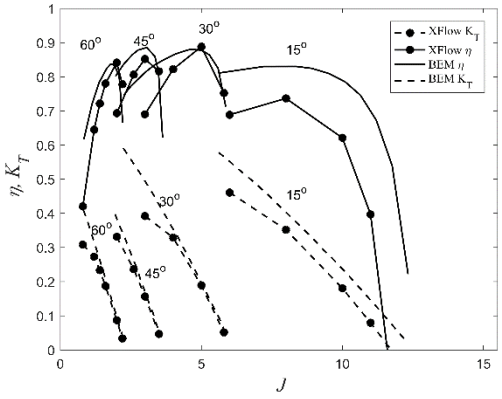

Figure 9. K_T and η in function of J_{eq}; h_0/c = 4; θ_0 = 15°, 30°, 45° and 60°.

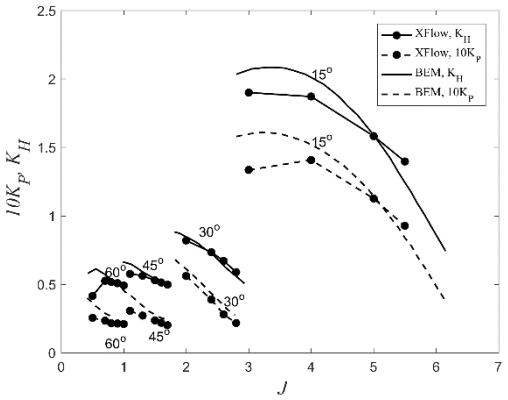

Figure 10. K_H and K_P in function of J_{eq}; h_0/c = 1; θ_0 = 15°, 30°, 45° and 60°.

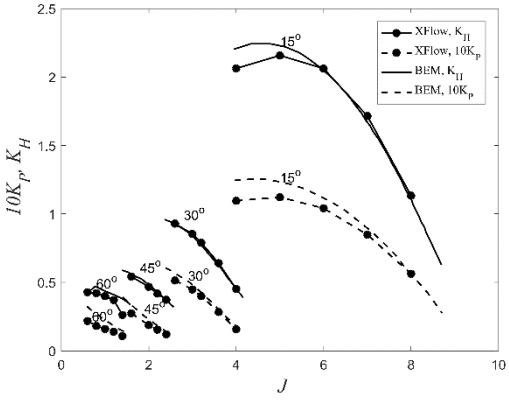

Figure 11. K_H and K_P in function of J_{eq}; h_0/c = 2; θ_0 = 15°, 30°, 45° and 60°.

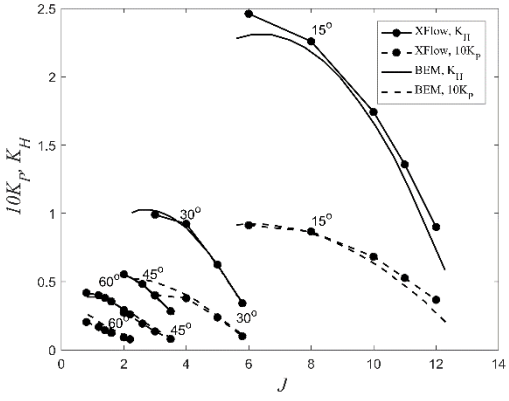

Figure 12. K_H and K_P in function of J_{eq}; h_0/c = 3; θ_0 = 15°, 30°, 45° and 60°.

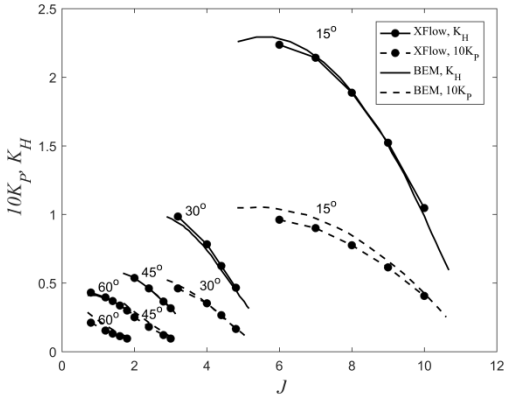

Figure 13. K_H and K_P in function of J_{eq}; h_0/c = 4; θ_0 = 15°, 30°, 45° and 60°.

5. Conclusion and Perspective

The viscous results agree well with the potential flow results. As expected, viscous results show lower efficiency in high flapping frequency zone. According to the viscous results, the possibility to use a flapping foil as a propulsion system is confirmed. The results show that the efficiency of a flapping foil propulsor can outperform a conventional screw propeller. The maximum efficiency is 90% for the viscous results and 87% for the inviscid results. For the case of 15° pitch amplitude, despite the lower efficiency compared with the other pitch amplitude cases, the propulsor can give an efficiency higher than 70% for a very wide range of equivalent advance ratios. Such propulsor can therefore be used like a controllable pitch propeller since it gives high efficiency for different sailing conditions i.e., different speeds and loads. However, from the point of view of mechanical complexity, the flapping foil seems to overcome the controllable pitch propellers.

References

[1] Rozhdestvensky K V and Ryzhov V A 2003 *Prog. Aerosp. Sci.* **39** pp 585-633
[2] Eloy C 2012 *J. Fluids Struct.* **7** pp 205-224
[3] Anderson J M, Streitlien K, Barrett D S and Triantafyllou M S 1998 *J. Fluid Mech.* **360** pp 41-72
[4] Blondeaux P, Fornarelli F, Guglielmini L, Triantafyllou M S and Verzicco R 2005 *Physics of Fluids* **17** 113601
[5] Read, Douglas A, Hover F S and Triantafyllou M S 2003 *J. Fluids Struct.* **17.1** pp 163-183.
[6] Floc'h F, Phoemsapthawee S, Laurens J M and Leroux J B 2012 *Ocean Eng.* **39** pp 56-61
[7] Xu G D, Xu W H and Dai J 2017 *Appl. Ocean Eng.* **63** pp 242-50
[8] Hover F S, Haugsdal O, Triantafyllou M S 2004 *J. Fluids Struct.* **19** pp 37-47
[9] Mantia M L and Dabnichki P 2011 *Appl. Math. Model.* **35** pp 979-990
[10] Belibassakis K A and Filippas E S 2015 *Appl. Ocean Res.* **52** pp 1-11
[11] Belibassakis K A and Politis G K 2013 *Ocean Eng.* **72** pp 227-40
[12] Politis G K and Tsarsitalidis V T 2014 *Ocean Eng.* **84** pp 98-123
[13] Phoemsapthawee S 2017 *Proc. of SIMMOD 2017* (Pattaya) pp 199-205
[14] Johnson A A 2006 *25th Army Science Conf.*
[15] XFlow 2016 *Computational fluid dynamics Theory guide* (Next Limit Technologies)
[16] XFlow 2016 *Computational fluid dynamics Validation guide* (Next Limit Technologies)
[17] Holman D M, Brionnaud R M, Martinez FJ and Mier-Torrecilla M 2012 *30th AIAA Applied Aerodynamics Conf.* (New Orleans)
[18] Sun X, Zhao L and Jiao Z 2016 *Proc. of 2016 IEEE Chinese Guidance, Navigation and Control Conf.* (Nanjing)